Received: 22 February 2021 | Revised: 3 August 2021 | Accepted: 6 September 2021

DOI: 10.1111/joa.13550

Journal of Anatomy | ANATOMICAL SOCIETY | WILEY

ORIGINAL PAPER

Virtual reconstruction of orbital floor defects using a statistical shape model

Mathieu Gass[1] | Marc Anton Füßinger[1] | Marc Christian Metzger[1] | Steffen Schwarz[1] | Johannes Daniel Bähr[1] | Leonard Brandenburg[1] | Julia Weingart[1] | Stefan Schlager[2]

[1]Department of Oral and Maxillofacial Surgery, Albert-Ludwigs University Freiburg, Freiburg, Germany

[2]Department of Physical Anthropology, Albert-Ludwigs-University Freiburg, Freiburg, Germany

Correspondence
Mathieu Gass, Department of Oral and Maxillofacial Surgery, Albert-Ludwigs University Freiburg, Hugstetterstr. 55, 79106 Freiburg, Germany.
Email: mathieu.gass@uniklinik-freiburg.de

Abstract

Purpose: The current standard in reconstructing defects of the orbital floor, by using the concept of mirroring, is time-consuming and ignores the natural asymmetry of the skull. By using a statistical shape model (SSM), the reconstruction can be automatized and improved in accuracy. The present study aims to show the possibilities of the virtual reconstruction of artificial defects of the orbital floor using an SSM and its potentials for clinical implementation.

Methods: Based on 131 unaffected CT scans of the midface, an SSM was created which contained the shape variability of the orbital floor. Nineteen midface CT scans, that were not included in the SSM, were manually segmented to establish ground truth (control group). Then artificial defects of larger and smaller sizes were created and reconstructed using SSM (Group I) and the gold standard of mirroring (Group II). Eventually, a comparison to the surface of the manual segmentation (control group) was performed.

Results: The proposed method of reconstruction using an SSM leads to more precise reconstruction results, compared with the conventional method of mirroring. Whereas mirroring led to the reconstruction errors of 0.7 mm for small defects and 0.73 mm for large defects, reconstruction using SSM led to deviations of 0.26 mm (small defect) and, respectively, 0.34 mm (large defect).

Conclusions: The presented approach is an effective and accurate method for reconstructing the orbital floor. In connection with modern computer-aided design and manufacturing, individual patient-specific implants could be produced according to SSM-based reconstructions and could replace current methods using manual bending techniques. By acknowledging the natural asymmetry of the human skull, the SSM-based approach achieves higher accuracy in reconstructing injured orbits.

KEYWORDS

computer-assisted surgery, orbital reconstruction, statistical shape model, trauma

Mathieu Gass and Marc-Anton Füssinger contributed equally.

1 | INTRODUCTION

Maxillofacial injuries are found to be one of the major health problems worldwide with epidemiology widely varying in different countries (Adi et al., 1990; Al-Khateeb & Abdullah, 2007; Bereket et al., 2015; Boffano et al., 2014). Maxillofacial fractures occur in a significant proportion of trauma patients because of the prominent and exposed position of the head and have been increasing over the past decades (Chrcanovic et al., 2012). Close proximity of various critical structures is a challenge in terms of functional, as well as esthetic outcomes, in craniomaxillofacial surgery (Wagner et al., 2015). Due to its exposed position and its limited bone thickness, orbital structures are involved in up to 40% of the maxillofacial trauma cases (Hoffmann et al., 1998), resulting in blowout fractures of zygomatic fractures involving the area of the orbital floor or the medial orbital wall, which may lead to diplopia and enophthalmos (Manolidis et al., 2002). To prevent such complications, the anatomical orbital structures have to be reconstructed true to original during the first surgery (Hammer & Prein, 1995). The development of preformed orbital implants based on topographical analysis of the orbital cavity was a milestone for the improvement of primary orbital reconstruction (Bittermann et al., 2014; Rana et al., 2014; Schramm et al., 2009; Unterhofer et al., 2017).

For most reconstruction purposes, computer-assisted surgery (CAS), based on computed tomography (CT) imaging data for three-dimensional visualization and virtual planning, is a well-established technique and offers great advantages for diagnosis, planning, therapy, and quality control (Aschendorff et al., 2009; Cornelius et al., 2015; Heiland et al., 2004; Levine et al., 2012; Metzger et al., 2013; Scolozzi, 2015; Strong et al., 2013; Wagner et al., 2015; Wilde et al., 2015). However, the combination of anatomical preformed orbital implants or patient specific implants with intraoperative cone-beam computer-tomography (CBCT) data acquisition led to an ongoing reduction of the need for navigation procedures.

In the classical planning process for unilateral deformations or defects, the unaffected side of the skull is segmented and mirrored onto the affected side based on the assumption of facial symmetry (Schmelzeisen et al., 2004). This procedure has been used as a gold standard over the last decades. With the actual gold standard still relying on mirroring the unaffected side, CAS is not suitable for patients being afflicted by bilateral defects (Gellrich et al., 2002; Schmelzeisen et al., 2004).

Recently, a semi-automatic method has been developed that is based on atlas segmentation (Metzger et al., 2013). Hereby, a virtual template model of the entire skull and its anatomical subregions is deformed to fit onto the individual dataset of a patient. The information of the atlas is fused with a patient's dataset and transformed to meet the individual's conditions. This procedure significantly reduces the time of preoperative planning (Metzger et al., 2013).

However, the conversion of CBCT data of the orbital cavity with its very thin bone into a virtual model is a challenging task. Segmentation without additional manual postprocessing is rarely suitable for virtual surgical planning.

In a recent study, a comparison of the existing atlas segmentation procedure (Brainlab, Feldkirchen, Germany) to a statistical shape model (SSM) was conducted to reconstruct a created defect of the zygomatic bone, showing a higher precision in the SSM group (Semper-Hogg et al., 2017).

The creation of the SSM in that study was based on 131 segmentations of CT scans from unaffected skulls. The dataset underwent a deformation on the created midface bony defect. To check for differences in accuracy, the reconstructed surfaces generated by the two methods were compared with the unaffected zygomatic region (Semper-Hogg et al., 2017). Similar studies testing the precision of SSM regarding reconstructions of large cranial defects as well as bilateral midfacial defects were performed by Fuessinger et al. and have shown the superiority over the mirrored reconstructions (Fuessinger et al., 2018, 2019). We are proposing a reconstruction procedure that is based on the following two steps: (1) globally fitting an SSM to the entire cranium and (2) an iterative procedure to apply a regularized deformation to fit the intact structure as close as possible. In this study, we evaluate the accuracy of said method and compare it to the current gold standard of mirroring the intact orbital floor to the affected side.

2 | MATERIALS AND METHODS

Ethical approval was obtained from the local ethics committee of Albert-Ludwigs-Universität Freiburg (450/15). The described research adhered to the tenets of the Declaration of Helsinki. Four main steps were performed to investigate our reconstruction method with the statistical shape model: First, a statistical shape model based on 131 segmentations of CT scans from unaffected sculls, with the orbital floor as a region of interest, was established. Then 19 orbital cavities were segmented manually and defects were created using Mesh Mixer (Autodesk, San Rafael, California, USA) and Blender 2.80 (Blender Foundation, Amsterdam, Netherlands) (Figure 2). Subsequently, the orbital floors were reconstructed virtually by using two methods. For a final comparison of both methods, an accuracy evaluation was done. Manual segmentations were performed using the open source software Slicer3d (Fedorov et al., 2012) and ITKSnap (Yushkevich et al., 2006). Atlas segmentations and the virtual reconstruction employing the mirroring procedure were carried out using iPlan CMF 3.0 (Brainlab, Feldkirchen, Germany). The virtual reconstruction based on the SSM, error assessment, and all subsequent statistical analyses were performed using RvtkStatismo (Schlager, 20152015), mesheR (Schlager, 2015), Morpho, and Rvcg (Schlager et al., 2017), which are extensions of the statistical–mathematical platform R (R Core Team, 2015) (Figure 1).

2.1 | Training data and testing data

The data consist of 150 cranial CT scans from patients, unaffected by osseous trauma, in the region of interest, taken in the course of medical treatment at Albert-Ludwigs-Universität Freiburg. The

Journal of Anatomy ANATOMICAL SOCIETY -WILEY

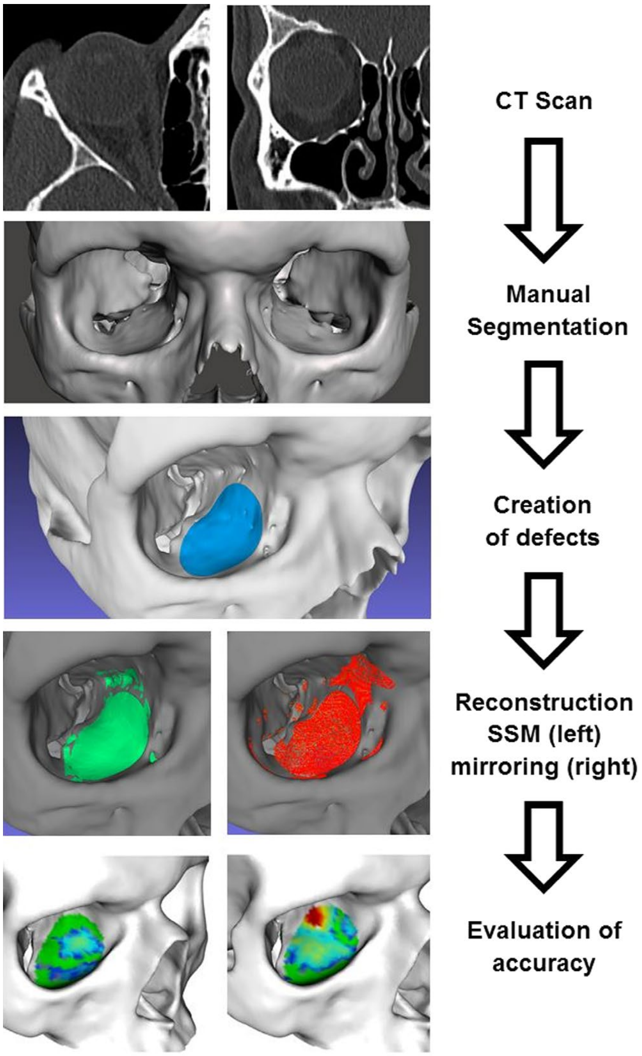

FIGURE 1 Proposed workflow for testing the different reconstruction methods

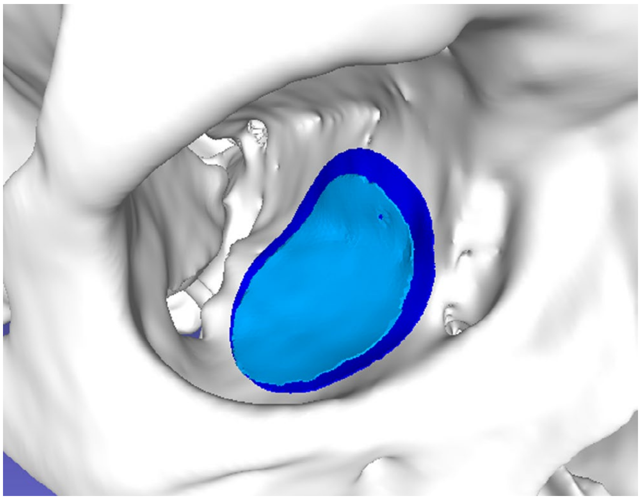

FIGURE 2 Size of the large defect shown in blue and size of the small defect shown in light blue

patient pool for the statistical shape model was identical to those used in Fuessinger et al. (2018, 2019) and Semper-Hogg et al. (2017). Of those, 131 individuals were used to generating a statistical shape model of the human cranium, capturing the shape variability of that structure in adults and representing the population of that region. Nineteen individuals were set aside as testing samples to evaluate the accuracy and precision of our proposed method as well as the conventional method of mirroring the unaffected side to the defect area.

2.2 | Statistical shape model revision

As the shape model, generated already for the former publications (Fuessinger et al., 2018, 2019; Semper-Hogg et al., 2017), was originally based on threshold-segmented image labels, those had to be amended in order to allow capturing the shape of the orbital floor more accurately. Therefore, the orbital cavities in all 131 patients, contributing to the shape model, had to be segmented semi-automatically, using the software iPlan CMF 3.0 (Brainlab, Feldkirchen, Germany). While the software allows for an automatic atlas segmentation of the human cranium, it often fails to correctly segment the inferior and medial walls of the orbital cavity due to the weak and ambiguous signal regarding the grey value distribution in this area. Those errors were corrected manually by trained surgeons and the shape in the reference population was updated accordingly, leading to a shape model where the variability of the orbital cavities is adequately represented.

2.3 | Preparation of testing sample and generation of virtual defects

Nineteen CT scans were set aside for testing purposes and to avoid statistical self-interference. In order to establish ground truth regarding the shape of the orbital cavities, the crania were the first threshold segmented and then a trained maxillofacial surgeon manually amended the orbital region. 3D surface meshes were generated from the resulting label images using a marching cube algorithm. Subsequently, virtual defects of two sizes were generated in the mediolateral wall in one of the orbital cavities by manually placing spheres (dimension large = 25 × 30 mm; dimension small = 20 × 25 mm) and removing the structures contained within those spheres. This procedure created circular defects (Figure 2).

2.4 | Virtual reconstruction using the proposed method SSM

The proposed virtual reconstruction procedure is similar to those introduced in Fuessinger et al. (2018, 2019) and Semper-Hogg et al. (2017). Regarding the final deformation in order to achieve a tight fit at the defects border and the surrounding structure, we replaced the generic thin-plate spline deformation with an iterative procedure that ensures the anatomical validity of the resulting orbital shape (see below).

The procedure can be outlined as follows:

1. Five anatomical landmarks, fronto-zygomale (bilateral), nasion, and the peak of the orbital funnels are placed in order to establish initial spatial correspondences between the SSM and the target mesh.
2. After a rigid alignment, the statistical shape model is globally fitted to the target resulting in the model instance that resembles the target cranium best regarding the overall shape. The outcome is an intact cranium globally adapted to the patient's cranial shape.
3. Fine-tuning: As in our previous publications, a point cloud is sampled on the SSM instance that is very dense in the region of interest (2000 coordinates inside the orbits) and sparser outside (1000 coordinates on the remainder of the cranium).
4. For each coordinate of the point cloud, the closest correspondence on the target shape is sought and evaluated regarding its distance and normal direction and unsuitable correspondences are discarded.
5. Based on the valid correspondences, the posterior mean shape, that is, the most likely shape satisfying those correspondences, is computed.
6. The result from Step 5 then deformed to the target correspondences using a thin-plate spline deformation.
7. Repeat Steps 4–6 until convergence.

Apart from the improved orbital shape representation and the individual placement of the defects in each of the 19 test models, Step 5 can be considered the main difference between our procedure in this paper and the method used in our preceding research using SSMs, where the globally fitted shape is directly warped to the target using the generic thin-plate spline deformation. While Step 4 results in a cranial surface model resembling the target shape regarding its overall appearance, Step 5 ensures a model instance that is as close to the valid correspondences in the region of interest as possible. The final gap between that model instance and the intact tissue surrounding the defect is then closed by a thin-plate spline deformation. This allows for a smooth fit at the defect borders while maintaining a shape as close to the shape distribution of a healthy population as possible.

2.5 | Virtual reconstruction using mirroring

The CT scans of the 19 patients constituting the testing sample were imported into the iPlan software (Brainlab, Feldkirchen, Germany) and the contralateral orbit was segmented employing the atlas segmentation method described by Metzger et al. (2013). The resulting 3D-surface mesh of the orbital cavity was then mirrored onto the contralateral defect orbit to allow reconstruction. As the full automatic mirroring process of the software ended in very imprecise reconstructions, manual adjustments regarding the final alignment of the mirrored orbit process were performed by a trained surgeon.

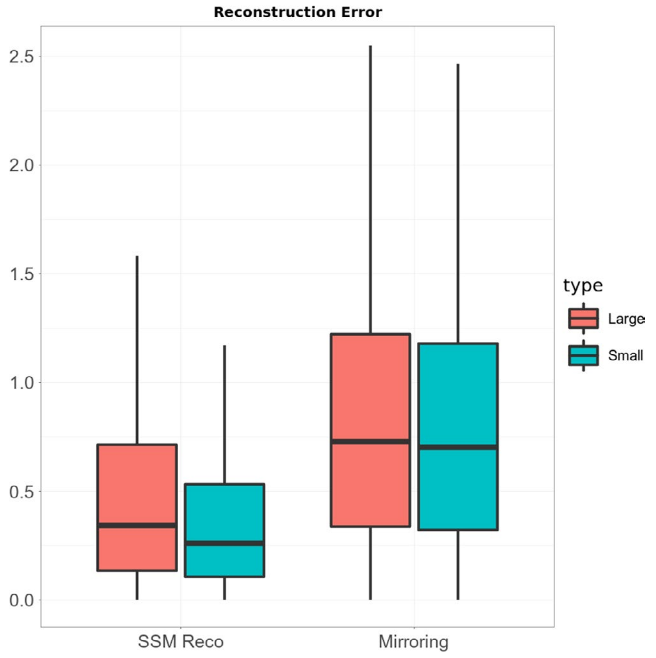

FIGURE 3 Reconstruction errors for large and small e defects in mm

2.6 | Evaluation

In order to evaluate the quality of the reconstruction methods, the deviations between the reconstructed area and the original unaffected state were analyzed. Using the manual segmentations as ground truth, for each vertex on the cranial facing surface of the removed part, the closest distance to the reconstructed surfaces was computed, resulting in a distribution of point to point distances. As error metrics, we computed the median and the percentage of vertices with an error below 1 mm.

3 | RESULTS

All defects of the orbital floor could be reconstructed with both methods. Figure 3 shows the accumulated error of the two reconstruction methods for small and large defects of the orbital floor. We focused on the upper surface of the orbital floor, as it is the crucial portion of the orbital cavity for the functional recreation of eye motility and unimpaired vision as well as esthetic outcome regarding enophthalmos (Manolidis et al., 2002). The median error using the mirroring technique for small defects amounts to 0.7 mm and for large defects 0.73 mm, whereas in the SSM-based reconstruction, the median errors amount to 0.26 mm for small defects and 0.34 mm for large defects (Figure 3). These differences also reflect in the percentages of vertices with errors below 1 mm. While the reconstructions based on mirroring exhibit a value of 69% in the large defects and 76% in the small defects, again the SSM reconstructions show a larger percentage of vertices with an error below 1 mm: 95% for small defects and 90% for large defects. Summarizing, we can assume that the SSM-based reconstruction leads to more accurate reconstructions of the orbital defects.

Figure 4 shows the reconstructions results summarized in a heat map, which shows the localization and extent of the reconstruction errors developed by the SSM and by mirroring.

4 | DISCUSSION

Our technique of reconstructing orbital floor defects with a statistical shape model represents an improved approach in computer-assisted surgery. The development of fitting patient-specific implants is a basic requirement in the treatment of orbital fractures (Bittermann et al., 2014; Rana et al., 2014; Schramm et al., 2009; Unterhofer et al., 2017). The restoration of the primary anatomic relations has a key role in the functional convalescence of the eye after trauma (Bittermann et al., 2014; Frohwitter et al., 2018; Hammer & Prein, 1995; Manolidis et al., 2002; Schönegg et al., 2018). CAS has shown to be an effective concept to improve the quality of surgical interventions (Dreizin et al., 2018; Jansen et al., 2018; Scolozzi, 2017). As already stated by several authors (Fuessinger et al., 2019; Semper-Hogg et al., 2017), the decrease of manual steps during the planning procedure is an important issue. Our proposed method is a viable and faster alternative to restore the orbital floor by simply clicking five anatomical landmarks on a segmented 3D model. Alignment of the mirrored unaffected side to the defective orbit requires manual interaction and is based on the physician's experience. Therefore, this method is prone to error. The required placement of the anatomical landmarks for fitting the patients' data to the SSM demands human interaction resulting in possible errors as well. Due to the proposed algorithm of fine-tuning, detection of the closest correspondence on the target shape, and the thin-plate spline deformation, automatization of the process is achieved and possible user-dependent errors are corrected subsequently. As the anatomical landmarks are only used to initialize the spatial alignment between SSM-space and the target space, the method is unsusceptible to inter- and intraobserver variability of the placement.

The importance of the clinical application in the orbital floor reconstruction is a stable and precise positioning of the PSI. In particular, the transition between the PSI and the healthy bony structures needs to be reconstructed smoothly to ensure a precise passive fit. Hence, we implemented a step to close the gap between the model instance and the intact tissue surrounding the defect using the thin-plate spline transformation in our algorithm.

Former publications concerning the reconstruction of bony defects of the skull already proposed the SSM as a functioning method and pointed out its clinical relevance: Fuessinger et al. (2019) performed the reconstruction of orbital floor defects by using the SSM with a mean error of 0.75 mm. The former study can be considered a pilot study to evaluate the general feasibility of our approach, as we used deformed versions of a template shape that did not involve manual segmentation, we can assume that it did not cover the entire variability of orbital floor shape as was the case in this study. Due to the increased accuracy of both, the SSM and the manually segmented testing data, the outcome of this study is more generalizable. Additionally, we introduced a fine-tuning step involving a model-guided deformation leading to a significant improvement in accuracy. Due to this added fine-tuning of the method and to the successful revision of the SSM regarding the orbital floor, we could decrease the mean reconstruction error to only 0.34 mm for large defects, respectively, 0.26 mm for small defects. In 17 of 19 reconstruction cases, the SSM was superior to the conventional mirroring technique. Furthermore, our study is, to our knowledge, the first one, which compares the reconstruction of orbital floor defects with an SSM-based method to the gold standard of mirroring. Apart from reducing subjectivity by user-interaction, our proposed method exhibits conceptual advantages when it comes to bilateral defects: while mirroring, for obvious reasons, is not able to reconstruct those defects, the SSM-based approach is a good alternative for assuming the anatomical starting position in patients with bilateral defects. The statistical shape model does not rely on one individual shape, but samples from a distribution generated from a healthy population based on 131 CT scans. The anatomy of the patient can sequentially be reconstructed based on the covariation between structures learned from that population, resulting in higher reconstruction accuracy. The current gold standard of mirroring assumes

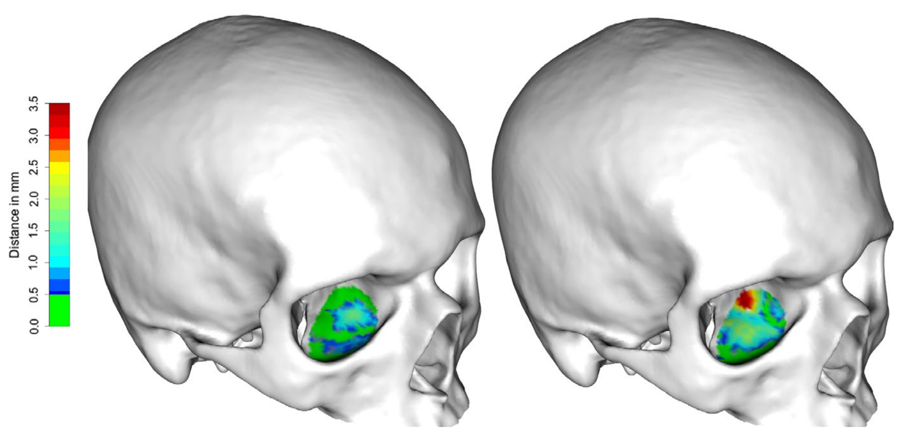

FIGURE 4 Reconstruction results of the SSM (left) and mirroring (right) and the corresponding colored reconstruction errors

the principle of symmetry of the skull, which could be disproved formerly (Metzger et al., 2007). The structured analysis of bony reconstructions of the orbital floor using mirroring techniques, performed by Metzger et al. (2007), showed reconstruction errors with a mean difference of 1.49 mm with a maximum modulus of 2.49 mm compared witth the original defect-free skull. The proposed concept of using a statistical shape model leads to higher accuracy and therefore enables more precise surgical treatment. Wagner et al. (2015) presented an extended method of mirroring concerning the whole skull for diffeomorphic registration and reconstruction of the skull. In comparison to the traditional mirroring technique, which only concerns a region similar to the defect in localization and somewhat larger, this method could not provide higher accuracy of reconstruction. Eventually it can be stated that reconstruction techniques using mirroring have conceptual disadvantages, due to cranial asymmetry resulting in higher discrepancies between the reconstructed model and the patient's original anatomy. Our proposed method provides a new approach, drawing upon the learned natural asymmetry and cranial shape variability. This knowledge appears to be an applicable and accurate tool for estimating the anatomy of missing or defective cranial parts. Modern computer-assisted design and manufacturing nowadays enable the production of printed patient-specific implants based on virtual 3D models (Scolozzi, 2017). In contrast, current reconstruction techniques are using standardized orbital meshes, which have to be bent pre- or intraoperatively to enable the best possible fit (Strong et al., 2013). These types of implants are positioned on top of the injured orbital floor, leading to an elevation of the eye of 0.4–0.5 mm. The difficulties of precise bending and intraoperative positioning of the mesh add to this conceptual shortcoming of the "inlay technique" and decrease the surgical accuracy. As the presented approach, using an SSM, provides an accurate 3D model of the orbit, a more detailed conversion of the precise reconstruction is required to benefit from this improvement. Future investigations therefore should address the development of implants using an inlay technique, which fit flush with the edges of the fractures and yield to a smooth and anatomically formed orbital floor without elevation of the eye by plate thickness or dead space between the orbital floor and the mesh.

5 | CONCLUSION

The presented approach is an effective and accurate method for reconstructing the orbital floor. In comparison to former publications (Fuessinger et al., 2019), the deviation error could be minimized, thanks to the revision of the underlying SSM and additional fine-tuning in the fitting procedure. Further investigations on implementing this method in our clinical practice for generating PSIs are currently planned.

Concluding it can be said that the proposed method offers a fast and cost-effective approach to virtually anatomical reconstructions and should be considered as a basic principle for the design of PSIs in the future.

CONFLICT OF INTEREST

The authors declare that they have no conflict of interest.

ETHICAL APPROVAL

All procedures performed in studies involving human participants were in accordance with the ethical standards of the institutional and/or national research committee and with the 1964 Helsinki declaration and its later amendments or comparable ethical standards.

ORCID

Mathieu Gass https://orcid.org/0000-0001-5015-9173
Marc Anton Füßinger https://orcid.org/0000-0003-4359-0744
Marc Christian Metzger https://orcid.org/0000-0002-4893-7594
Steffen Schwarz https://orcid.org/0000-0003-3666-6667
Johannes Daniel Bähr https://orcid.org/0000-0003-0125-7193
Leonard Brandenburg https://orcid.org/0000-0003-4697-5287
Julia Weingart https://orcid.org/0000-0002-1438-9745
Stefan Schlager https://orcid.org/0000-0001-6493-9250

REFERENCES

Adi, M., Ogden, G.R. & Chisholm, D.M. (1990) An analysis of mandibular fractures in Dundee, Scotland (1977 to 1985). *British Journal of Oral and Maxillofacial Surgery*, 28(3), 194–199.

Al-Khateeb, T. & Abdullah, F.M. (2007) Craniomaxillofacial injuries in the United Arab Emirates: a retrospective study. *Journal of Oral and Maxillofacial Surgery*, 65(6), 1094–1101.

Aschendorff, A., Maier, W., Jaekel, K., Wesarg, T., Arndt, S., Laszig, R. et al. (2009) Radiologically assisted navigation in cochlear implantation for X-linked deafness malformation. *Cochlear Implants International*, 10(sup1), 14–18.

Bereket, C., Şener, İ., Şenel, E., Özkan, N. & Yilmaz, N. (2015) Incidence of mandibular fractures in black sea region of Turkey. *Journal of Clinical and Experimental Dentistry*, 7(3), e410–e413.

Bittermann, G., Metzger, M.C., Schlager, S., Lagreze, W.A., Gross, N., Cornelius, C. et al. (2014) Orbital reconstruction: prefabricated implants, data transfer, and revision surgery. *Facial Plastic Surgery*, 30(5), 554–560.

Boffano, P., Kommers, S.C., Karagozoglu, K.H. & Forouzanfar, T. (2014) Aetiology of maxillofacial fractures: a review of published studies during the last 30 years. *British Journal of Oral and Maxillofacial Surgery*, 52(10), 901–906.

Chrcanovic, B.R., Abreu, M.H., Freire-Maia, B. & Souza, L.N. (2012) 1,454 mandibular fractures: a 3-year study in a hospital in Belo Horizonte, Brazil. *Journal of Cranio-Maxillo-Facial Surgery*, 40(2), 116–123.

Cornelius, C.P., Smolka, W., Giessler, G.A., Wilde, F. & Probst, F.A. (2015) Patient-specific reconstruction plates are the missing link in computer-assisted mandibular reconstruction: a showcase for technical description. *Journal of Cranio-Maxillo-Facial Surgery*, 43(5), 624–629.

Dreizin, D., Nam, A.J., Hirsch, J. & Bernstein, M.P. (2018) New and emerging patient-centered CT imaging and image-guided treatment paradigms for maxillofacial trauma. *Emergency Radiology*, 25(5), 533–545.

Fedorov, A., Beichel, R., Kalpathy-Cramer, J., Finet, J., Fillion-Robin, J.-C., Pujol, S. et al. (2012) 3D Slicer as an image computing platform for the Quantitative Imaging Network. *Magnetic Resonance Imaging*, 30(9), 1323–1341.

Frohwitter, G., Wimmer, S., Goetz, C., Weitz, J., Ulbig, M., Kortuem, K.U. et al. (2018) Evaluation of a computed-tomography-based assessment scheme in treatment decision-making for isolated orbital floor fractures. *Journal of Cranio-Maxillofacial Surgery*, 46(9), 1550–1554.

Fuessinger, M.A., Schwarz, S., Cornelius, C.-P., Metzger, M.C., Ellis, E., Probst, F. et al. (2018) Planning of skull reconstruction based on a statistical shape model combined with geometric morphometrics. *International Journal of Computer Assisted Radiology and Surgery*, 13(4), 519–529.

Fuessinger, M.A., Schwarz, S., Neubauer, J., Cornelius, C.-P., Gass, M., Poxleitner, P. et al. (2019) Virtual reconstruction of bilateral midfacial defects by using statistical shape modeling. *Journal of Cranio-Maxillofacial Surgery*, 47(7), 1054–1059.

Gellrich, N.-C., Schramm, A., Hammer, B., Rojas, S., Cufi, D., Lagrèze, W. et al. (2002) Computer-assisted secondary reconstruction of unilateral posttraumatic orbital deformity. *Plastic and Reconstructive Surgery*, 110(6), 1417–1429.

Hammer, B. & Prein, J. (1995) Correction of post-traumatic orbital deformities: operative techniques and review of 26 patients. *Journal of Cranio-Maxillo-Facial Surgery*, 23(2), 81–90.

Heiland, M., Schmelzle, R., Hebecker, A. & Schulze, D. (2004) Intraoperative 3D imaging of the facial skeleton using the SIREMOBIL Iso-C3D. *Dentomaxillofacial Radiology*, 33(2), 130–132.

Hoffmann, J., Cornelius, C.P., Groten, M., Pröbster, L., Pfannenberg, C. & Schwenzer, N. (1998) Orbital reconstruction with individually copy-milled ceramic implants. *Plastic and Reconstructive Surgery*, 101(3), 604–612.

Jansen, J., Schreurs, R., Dubois, L., Maal, T.J.J., Gooris, P.J.J. & Becking, A.G. (2018) The advantages of advanced computer-assisted diagnostics and three-dimensional preoperative planning on implant position in orbital reconstruction. *Journal of Cranio-Maxillofacial Surgery*, 46(4), 715–721.

Levine, J.P., Patel, A., Saadeh, P.B. & Hirsch, D.L. (2012) Computer-aided design and manufacturing in craniomaxillofacial surgery: the new state of the art. *Journal of Craniofacial Surgery*, 23(1), 288–293.

Manolidis, S., Weeks, B.H., Kirby, M., Scarlett, M. & Hollier, L. (2002) Classification and surgical management of orbital fractures: experience with 111 orbital reconstructions. *Journal of Craniofacial Surgery*, 13(6), 726–738.

Metzger, M.C., Bittermann, G., Dannenberg, L., Schmelzeisen, R., Gellrich, N.-C., Hohlweg-Majert, B. et al. (2013) Design and development of a virtual anatomic atlas of the human skull for automatic segmentation in computer-assisted surgery, preoperative planning, and navigation. *International Journal of Computer Assisted Radiology and Surgery*, 8(5), 691–702.

Metzger, M.C., Hohlweg-Majert, B., Schön, R., Teschner, M., Gellrich, N.-C., Schmelzeisen, R. et al. (2007) Verification of clinical precision after computer-aided reconstruction in craniomaxillofacial surgery. *Oral Surgery, Oral Medicine, Oral Pathology, Oral Radiology, and Endodontology*, 104(4), e1–e10.

R Core Team. *R: a language and environment for statistical computing*. Vienna, Austria: R Foundation for Statistical Computing; 2015. https://www.R-project.org/.

Rana, M., Essig, H., Rücker, M. & Gellrich, N.C. (2014) Development and demonstration of a novel computer planning solution for predefined correction of enophthalmos in anophthalmic patients using prebended 3D titanium-meshes–a technical note [published correction appears in. *Journal of Oral and Maxillofacial Surgery*, 70(11), e631–e638.

Schlager, S. mesheR: meshing operations on triangular meshes. 2015. http://github.com/zarquon42b/mesheR

Schlager, S. (2015) RvtkStatismo: integrating statismo and R using the vtkStandardMeshRepresenter. http://github.com/zarquon42b/RvtkStatismo. Accessed 2015.

Schlager, S. (2017) Morpho and Rvcg – shape analysis in R. In: Zheng, G., Li, S. & Szekely, G. editors. *Stat Shape Deform Anal*. Academic Press, pp. 217–256.

Schmelzeisen, R., Gellrich, N.C., Schoen, R., Gutwald, R., Zizelmann, C. & Schramm, A. (2004) Navigation-aided reconstruction of medial orbital wall and floor contour in cranio-maxillofacial reconstruction. *Injury*, 35(10), 955–962.

Schönegg, D., Wagner, M., Schumann, P., Essig, H., Seifert, B., Rücker, M. et al. (2018) Correlation between increased orbital volume and enophthalmos and diplopia in patients with fractures of the orbital floor or the medial orbital wall. *Journal of Cranio-Maxillofacial Surgery*, 46(9), 1544–1549.

Schramm, A., Suarez-Cunqueiro, M.M., Rücker, M., Kokemueller, H., Bormann, K.-H., Metzger, M.C. et al. (2009) Computer-assisted therapy in orbital and mid-facial reconstructions. *The International Journal of Medical Robotics and Computer Assisted Surgery*, 5(2), 111–124.

Scolozzi, P. (2015) Computer-aided design and computer-aided modeling (CAD/CAM) generated surgical splints, cutting guides and custom-made implants: which indications in orthognathic surgery? *Revue de Stomatologie, de Chirurgie Maxillo-faciale et de Chirurgie Orale*, 116(6), 343–349.

Scolozzi, P. (2017) Applications of 3D orbital computer-assisted surgery (CAS). *Journal of Stomatology, Oral and Maxillofacial Surgery*, 118(4), 217–223.

Semper-Hogg, W., Fuessinger, M.A., Schwarz, S., Ellis, E., Cornelius, C.-P., Probst, F. et al. (2017) Virtual reconstruction of midface defects using statistical shape models. *Journal of Cranio-Maxillofacial Surgery*, 45(4), 461–466.

Strong, E.B., Fuller, S.C., Wiley, D.F., Zumbansen, J., Wilson, M.D. & Metzger, M.C. (2013) Preformed vs intraoperative bending of titanium mesh for orbital reconstruction. *Otolaryngology–Head and Neck Surgery*, 149(1), 60–66.

Unterhofer, C., Wipplinger, C., Verius, M., Recheis, W., Thomé, C. & Ortler, M. (2017) Reconstruction of large cranial defects with polymethyl-methacrylate (PMMA) using a rapid prototyping model and a new technique for intraoperative implant modeling. *Neurologia i Neurochirurgia Polska*, 51(3), 214–220.

Wagner, M.E., Lichtenstein, J.T., Winkelmann, M., Shin, H.O., Gellrich, N.C. & Essig, H. (2015) Development and first clinical application of automated virtual reconstruction of unilateral midface defects. *Journal of Cranio-Maxillofacial Surgery*, 43(8), 1340–1347.

Wilde, F., Winter, K., Kletsch, K., Lorenz, K. & Schramm, A. (2015) Mandible reconstruction using patient-specific pre-bent reconstruction plates: comparison of standard and transfer key methods. *International Journal of Computer Assisted Radiology and Surgery*, 10(2), 129–140.

Yushkevich, P.A., Piven, J., Hazlett, H.C., Smith, R.G., Ho, S., Gee, J.C. et al. (2006) User-guided 3D active contour segmentation of anatomical structures: significantly improved efficiency and reliability. *NeuroImage*, 31(3), 1116–1128.

How to cite this article: Gass, M., Füßinger, M.A., Metzger, M.C., Schwarz, S., Bähr, J.D., Brandenburg, L., et al (2022) Virtual reconstruction of orbital floor defects using a statistical shape model. *Journal of Anatomy*, 240, 323–329. https://doi.org/10.1111/joa.13550